

Spectral Investigations on N-(2-Methylthiophenyl)-2-Hydroxy-1-Naphthaldimine by Silver Nanoparticles: Quenching

P. Manikandan · V. Ramakrishnan

Received: 30 July 2010 / Accepted: 18 October 2010 / Published online: 4 November 2010
© Springer Science+Business Media, LLC 2010

Abstract The photo—physical properties of N-(2-methylthiophenyl)-2-hydroxy-1-naphthaldimine (NMTHN) on silver nano particles have been investigated using optical absorption and fluorescence emission techniques. Silver nanoparticles of different sizes have been prepared by two different methods. The increases in size of the silver nanoparticles cause a decrease in the quenching of fluorescence of NMTHN. Stern–Volmer quenching constants and the association constants have also been calculated.

Keywords N-(2-methylthiophenyl)-2-hydroxy-1-naphthaldimine · Silver nanoparticle · Optical absorption · Fluorescence emission · Fluorescence quantum yield

Introduction

The derivatives of 2-hydroxy-1-naphthaldehyde can be embodied into a pesticide composition which is provided in the form of emulsions suspensions, dusts and aerosol sprays. In general such compositions are used in pesticide preparations [1]. Schiff bases are considered as a very important class of organic compounds. Schiff bases have been extensively studied and used as ligands in many complex species [2]. Condensation of primary amines with aldehydes or ketones yield schiff bases containing imine (C=N) function. Schiff base molecules decorated with necessary groups are important in various

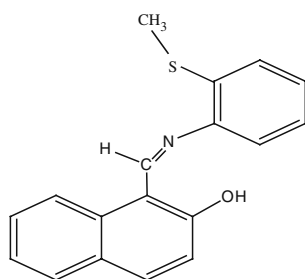
branches of chemistry as potential biomimics. 2-hydroxy-1-naphthaldehyde schiff bases ligands used in the field of coordination chemistry of metal ions including those present in biological systems [3]. Ortho hydroxyl Schiff bases, which are widely used as chelating agents, are relevant due to the possibility of finding them in the solid state and or in solution as keto-amine or phenol amine tautomers and their connections with phototropism and thermochromism [4].

Nanotechnology deals with processes that take place on the nanometer scale, that is, from approximately 1 to 100 nm. Properties of metal nanoparticles are different from those of bulk materials made from the same atoms [5]. The integration of nanotechnology with biology and medicine is expected to produce major advances in molecular diagnostics, therapeutics and bioengineering [6, 7]. These properties strongly depend on the particle size; inter particle distance, nature of the protecting organic shell and shape of the nanoparticles. The extremely small size of nanoparticles compared with the bulk material are easily interacting with other particles and increases their antibacterial efficiency. Metal nanoparticle—fluorophore structure is used for producing new material with optical and photochemical properties. Fluorescence quenching is a process which decreases the fluorescence intensity of a given substance. Fluorescence quenching may also result from a photo induced electron- transfer process between the excited dye and the metal nanoparticle. The interaction with the dye and excited-state surface reactions may lead to morphological changes of the metal nanoparticles [8]. Fluorescence resonance energy transfer is a photo physical process and occurs via intermolecular energy transfer mechanism where energy that is absorbed by fluorescent molecule is transferred non-radiatively to a second fluorescent molecule [9]. In the present work the effect of silver nanoparticles on N-

P. Manikandan · V. Ramakrishnan (✉)
Department of Laser studies, School of Physics,
Madurai Kamaraj University,
Madurai 625021, India
e-mail: vr.optics1@gmail.com

P. Manikandan
e-mail: manifishi@yahoo.com

Fig. 1 Structural formula of N-(2-methylthiophenyl)-2-hydroxy-1-naphthalimine



(2-methylthiophenyl)-2-hydroxy-1-naphthalimine (Fig. 1) has been investigated using optical absorption and fluorescence emission techniques.

Experimental

Material

2-hydroxy-1-naphthaldehyde (1.72 g, 10 mmol) was dissolved in alcohol and treated with an alcoholic solution of 2-(methylthio) aniline (1.39 g, 10 mmol). The content of the above solution was kept at room temperature over night. The formation of Schiff base takes place slowly with good yield. The pure brownish yellow crystals of the Schiff base was filtered, washed with alcohol and dried.

Procedure to Synthesis Silver Nanoparticles

The silver nanoparticles used in this study were synthesized by two different methods.

In the first method silver sol was prepared according to Creighton method [10]. In brief 2 ml of silver nitrate

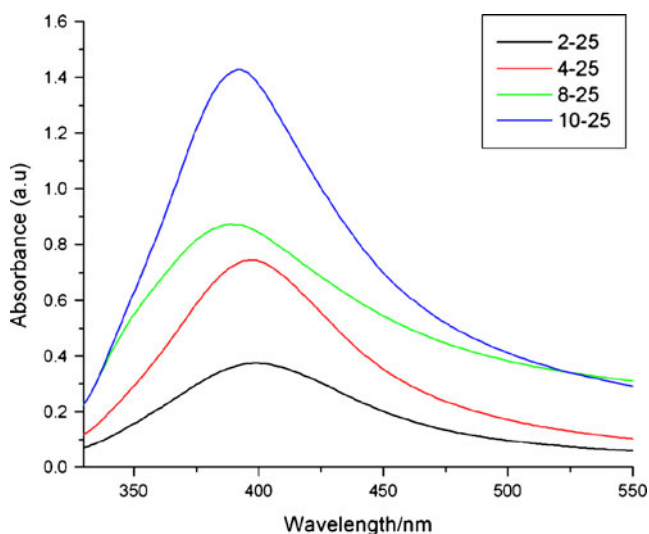


Fig. 2 Optical absorption spectra of silver nanoparticles prepared by first method (2:25; 2 ml Silver Nitrate solution, 25 ml Sodium Borohydride solution)

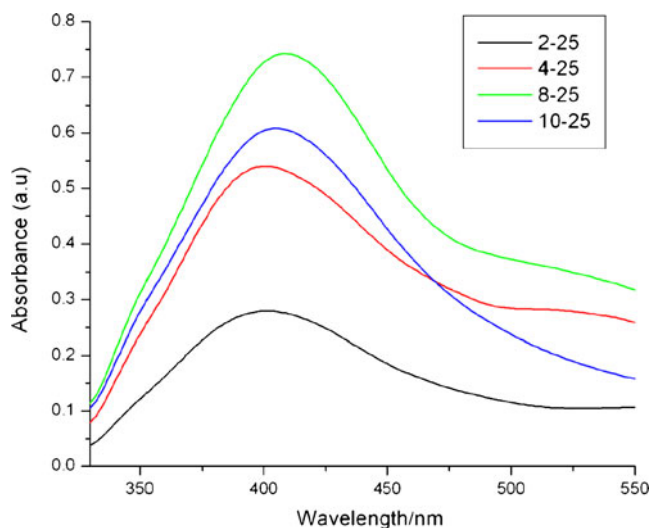


Fig. 3 Optical absorption spectra of silver nanoparticles prepared by second method (2:25; 2 ml Silver Nitrate solution, 25 ml Sodium Borohydride solution)

solution (0.6 mM) was added drop wise to 25 ml of sodium borohydride solution (1.2 mM) with vigorous stirring. It was repeated for different volume of silver nitrate (2, 4, 8 and 10 ml) at constant volume of sodium borohydride solution (25 ml). Both the solutions were chilled to ice temperature. In the second method, in the presence of ultrasonic field, 2 ml of silver nitrate solution (0.6 mM) was added drop wise to 25 ml of sodium borohydride solution (1.2 mM). It was repeated for different volume of silver nitrate solution (2, 4, 8 and 10 ml) at constant volume of sodium borohydride solution (25 ml). The ultrasonic treatment time was 1 h 30 min for all the cases. Both the solutions were chilled to 0 °C. Milli-Q water was used to synthesize the silver nanoparticles.

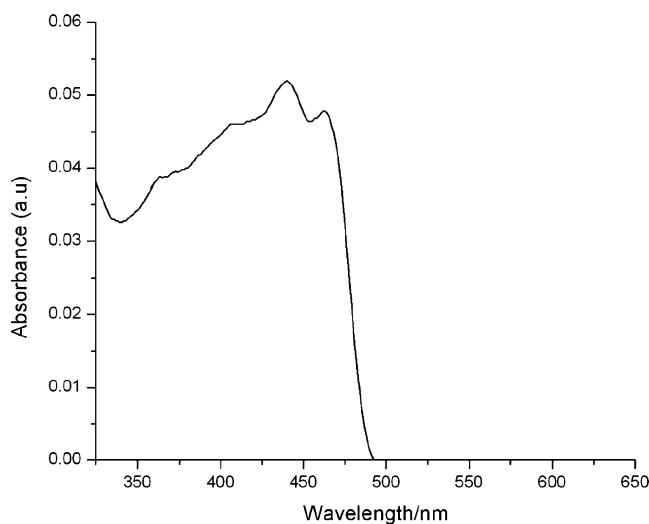


Fig. 4 Absorption spectrum of NMTN in methanol

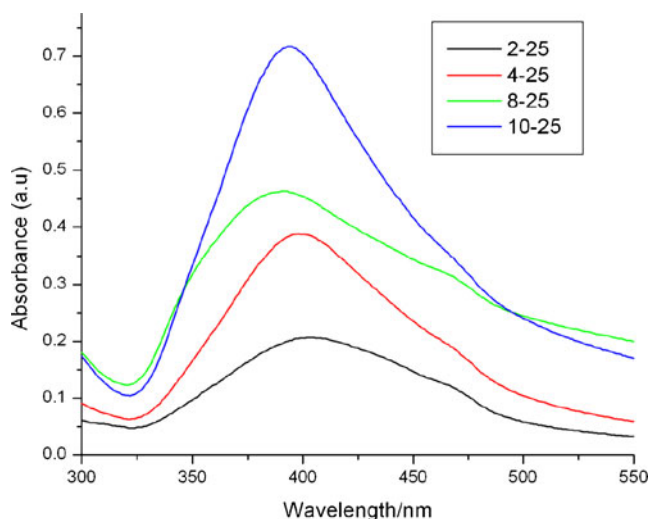


Fig. 5 Absorption spectra of NMTHN in silver nanoparticles prepared by first method

The concentration of NMTHN in methanol was 0.01 mM. Silver nanoparticles and NMTHN have been taken is 1:1 volume ratio.

Apparatus

Optical absorption spectra were recorded using a Shimadzu UV-2450 UV–visible spectrophotometer. Shimadzu RF-5301PC Spectrofluorophotometer was used to record fluorescence spectra. All the measurements were carried out at room temperature.

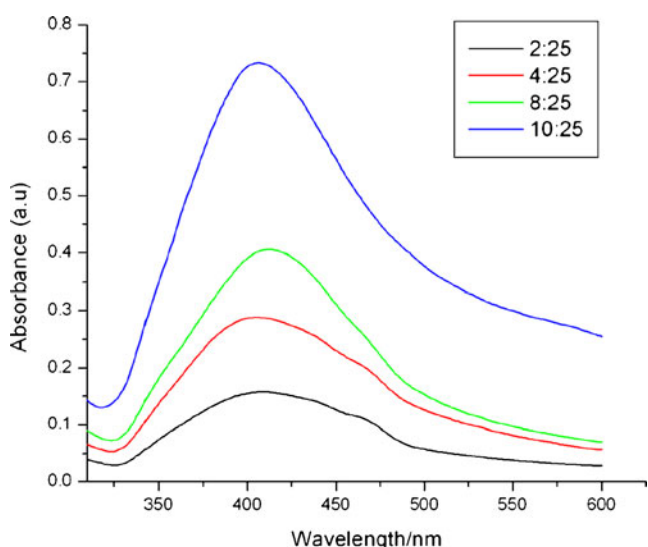


Fig. 6 Absorption spectra of NMTHN in silver nanoparticles prepared by second method

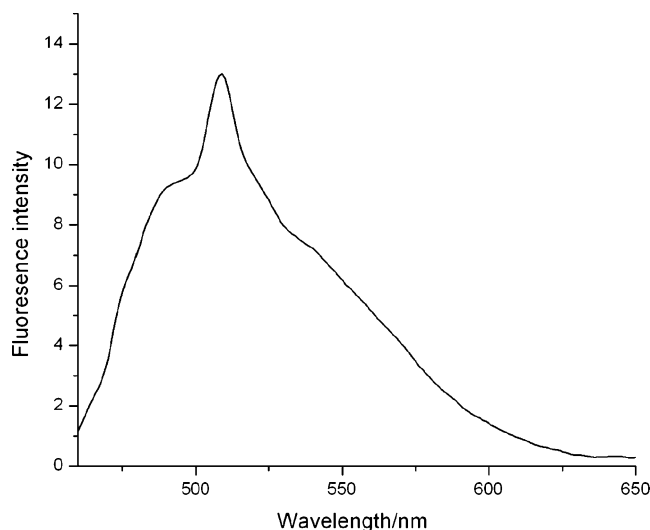


Fig. 7 Fluorescence spectrum of NMTHN in methanol

Results and Discussion

Determination of Silver Nanoparticle Size

Absorption spectra of metal colloidal dispersions exhibit broad bands in the UV-visible range due to the excitation of plasma resonances or interband transitions. The absorption and the scattering of light spectra from the small particles of the solid have more than one resonance peak caused by several different mechanisms such as plasmons (free electrons), phonons (lattice vibrations) and excitons (electron-hole pairs). For small metal particles the more interesting peaks are those caused by plasmons. The ratio of the surface area to the volume in the small particles is

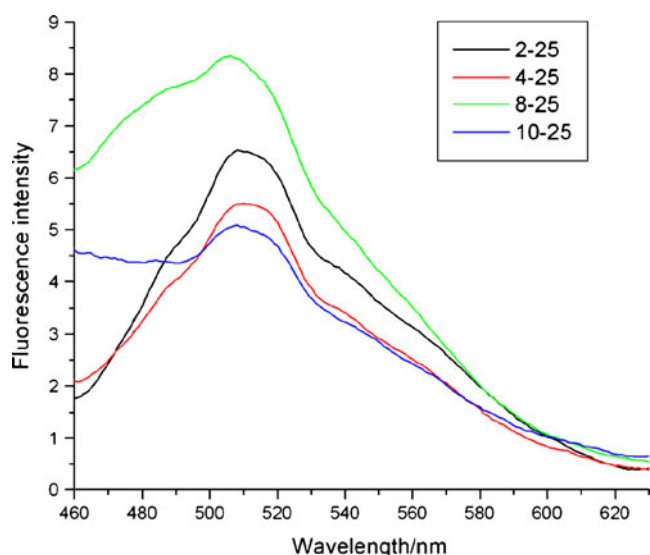


Fig. 8 Fluorescence spectra of NMTHN in silver nanoparticles prepared by first method

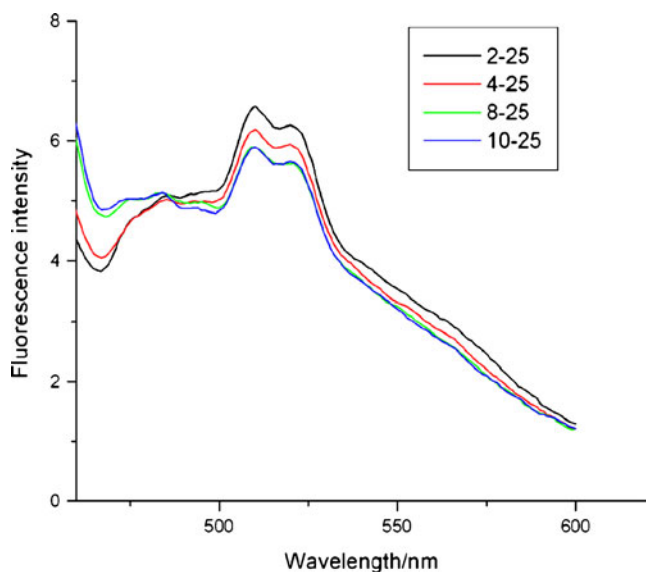


Fig. 9 Fluorescence spectra of NMTHN in silver nanoparticles prepared by second method

greater than the bulk material; consequently, one can state that the resonance is caused by the surface plasmons of the particles. The surface plasmon resonance can be thought of as the coherent motion of the conduction-band electrons caused by interaction with an electromagnetic field. The plasmon resonance is the strongest and shifted into the visible part of the electromagnetic spectrum for the noble metals [copper, silver, and gold]. The position and intensity of the metal surface-plasmon absorption band depends strongly on particle size, and the optical and electronic properties of the medium surrounding the particles. The chemisorption of various nucleophiles has two opposing effects on the absorption spectra of colloidal silver. First, the increase in electron density in the particles that results

from electron donation by the adsorbed molecule, leads to a blue shift of the plasmon band. Second, the formation of a dipole on the surface of the particles causes a red shift of the band. For various silver organic molecular systems the second effect was shown to dominate [11].

The colloidal particle size can be determined from the Mie theory. This theory was developed for particles in spherical shape only. If the particle dimensions are smaller than the mean free path of the conduction electrons, collisions of these electrons with the particle surface takes place [12]. The metal colloidal solution color mainly depends on the particle size, but also on the shape, the refractive index of the surrounding media and the separation between the particles. If there is any shift in the surface plasmon resonance peak, above parameters will change [13].

The complex relative permittivity of the metal is $\epsilon = \epsilon' + i\epsilon''$. The extinction cross section can be expressed as,

$$C_{ext} = \frac{24\pi^2 R^3 \epsilon_m^{\frac{3}{2}}}{\lambda} \cdot \frac{\epsilon''}{(\epsilon' + 2\epsilon_m)^2 + \epsilon''^2}$$

Where R is the radius of the particle, λ is the wavelength of light in the media and ϵ_m the dielectric constant of the surrounding medium. For these free-electron metals ϵ'' is fairly constant in the UV-vis range and as is well-known, a maximum in the absorption thus occurs when, $\epsilon' = -2\epsilon_m$ due to the dipole plasma resonance of the spheres [14].

Fluorescence Quantum Yield

The fluorescence quantum yield (ϕ) of the sample in terms of the reference sample (ϕ_r) is $\phi_X = \phi_r \frac{A_r \lambda_r}{A_x \lambda_x} \cdot \frac{I_r \lambda_r}{I_x \lambda_x} \cdot \left(\frac{D_x}{D_r}\right)$. Here, $A_x \lambda_x$ & $A_r \lambda_r$ are absorbance values at the exciting wavelength, $I_x \lambda_x$ & $I_r \lambda_r$ are intensities of exciting light at wavelength (λ) and D_x & D_r are the integrated area under

Table 1 Particle size and Quantum yield values of NMTHN in Silver nanoparticles

	Volume of aqueous (ml) AgNO ₃ : NaBH ₄	Particle size (radius) (nm)	Quantum yield (ϕ)
First method			
S.No.			
1	2:25	25.3	1.275
2	4:25	31.0	0.660
3	8:25	33.6	0.661
4	10:25	37.1	0.385
Second method			
S.No.			
1	2:25	22.6	1.314
2	4:25	26.4	0.567
3	8:25	30.4	0.742
4	10:25	35.0	0.289

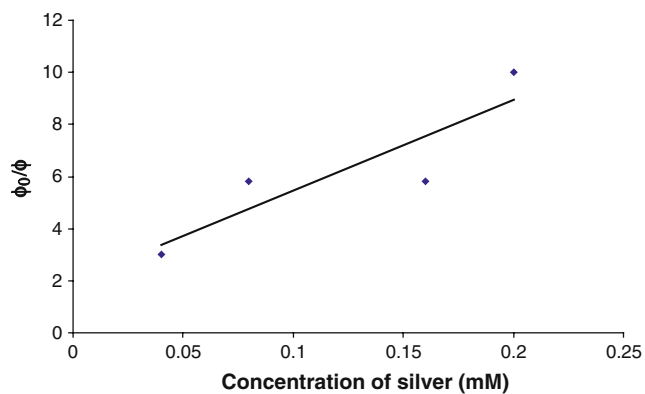


Fig. 10 Variation of ϕ_0/ϕ vs. concentration of silver (First method)

the emission spectrum. Here x, r is the unknown & reference sample respectively [15]. In which 1, 4-dihydroxy-2, 3-dimethyl-9, 10- anthraquinone in methanol was used as fluorescence standard ($\phi_r=1.0836$) [16]. In the present case the fluorescence quantum yield of NMTHN in methanol was found to be 3.8441.

Optical Absorption and Fluorescence Emission Studies

In the present case, the silver nanoparticle exhibits a plasmon band between 390–400 nm (Figs. 2 and 3). Their origin is attributed to the collective oscillation of the free conduction electrons induced by an interacting electromagnetic field [17]. This result confirms that the shape of the nanoparticles are spherical.

In the present work, the size effect and the quenching of metal nanoparticles on NMTHN are investigated using absorption and emission spectra. Different sizes of silver nanoparticle are calculated. The absorption spectra of NMTHN in methanol and the absorption spectra of NMTHN in metallic silver colloids are shown in Figs. 4, 5 and 6. The fluorescence emission spectra of NMTHN in

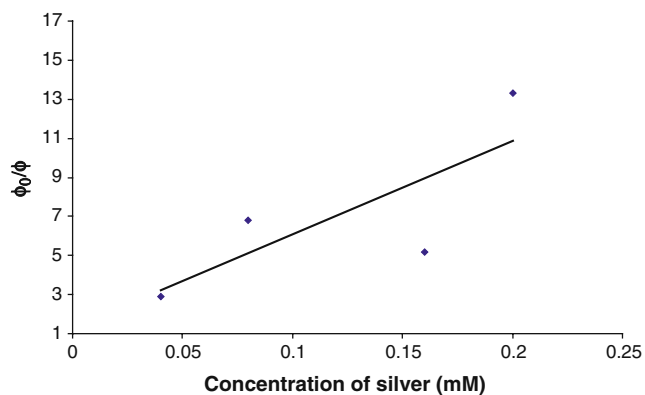


Fig. 11 Variation of ϕ_0/ϕ vs. concentration of silver (Second method)

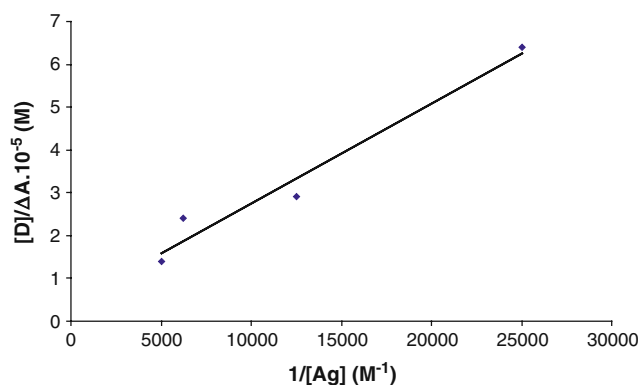


Fig. 12 Variation of $[D]/\Delta A$ vs. $1/[Ag]$ for NMTHN in Silver nanoparticles prepared by first method

methanol and the fluorescence emission spectra of NMTHN in silver nanoparticles are shown in Figs. 7, 8 and 9. The different sizes of silver nanoparticle and the fluorescence quantum yield of NMTHN are shown in Table 1.

Metallic surfaces interact with the fluorophores by the mechanisms that can cause quenching, increased rates of excitation, and/or increased quantum yields. Some fluorophores, particularly those with some conformational freedom, display increased quantum yields in rigid environments. Typically, a rigid environment results in decreased rates of nonradiative decay and thus longer lifetimes. Metallic colloids are known to be strongly scattering. Fluorophores with their transition dipoles oriented parallel to a silver surface are expected to have shorter lifetimes than those with a perpendicular orientation [18].

The excited singlet state of the donor transfers an electron to the acceptor into yield a charge separated state, which returns to the ground state by charge recombination [19]. A molecule chemisorbed on the metal surface will share some of its electrons with the metal and for such

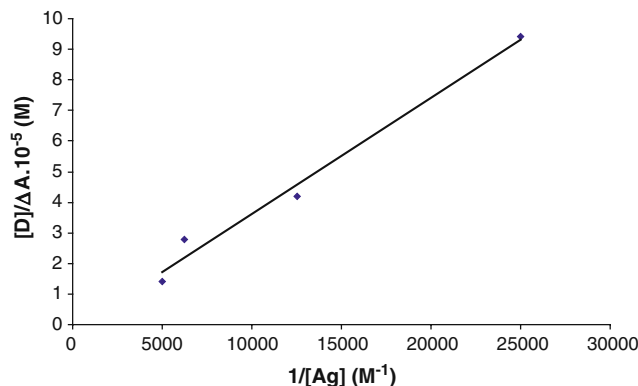


Fig. 13 Variation of $[D]/\Delta A$ vs. $1/[Ag]$ for NMTHN in Silver nanoparticles prepared by second method

systems one would in general expect charge transfer to have a strong influence on a variety of dynamical process such as quenching of vibrational or electronic excitations, dissociation reactions and sticking [20].

The rate of energy transfer of the forster theory mainly depends on the overlap of the donor emission and absorption spectrum, the quantum yield of the donor, the orientation of the donor and acceptor transition dipoles and the distance between the donor and acceptor transition dipoles [9]. Self-assembled monolayers on Au surfaces have also been applied to organize micro structured electronic circuits on nonconducting surfaces [21]. These reports show that it is, indeed, possible to generate sufficiently long-lived excited states in self-assembled monolayers functionalized with photo reactive moieties that effective photochemical modification of the metal-dielectric interface can be observed. They also demonstrate that photochemistry can be a useful tool in characterizing the local environment of covalently attached molecules present as monolayers on metal surfaces [22].

The assembly of ordered metal nanoparticles on solid supports attracts substantial research efforts as a consequence of their unique electronic and optical properties. The assembly of Au or Ag-colloid monolayers on glass or conductive glass supports has been accomplished by the self-organization of the metal particles associated with the solid supports [23]. Quenching of the excited state by the conductive metal surface that result in energy transfer to the metal surface has been reported earlier. The probability of this Forster energy transfer depends on the overlap of the fluorescence band of the dye molecule with the absorption band of the acceptor. The surface plasmon efficiently acts as an energy acceptor even at a distance of 1 nm between dye molecules and silver film surfaces. The interaction with the dye and excited state surface reactions may lead to morphological changes of the silver nano-particles.

The static and dynamic quenching constants have been calculated using Stern–Volmer equation which is generally written as $\phi_0/\phi = 1 + K_{sv}[A_g]$. Here $K_{SV} = K_S + K_D$ [24], ϕ_0 & ϕ are the fluorescence quantum yield of NMTHN in the absence and the presence of quencher [Ag], and K_S & K_D are the static and dynamic quenching constants respectively. Figures 10 and 11 shows the plot of ϕ_0/ϕ vs. silver concentration. The plot is considered as linear with $K_{SV} = 3.49 \times 10^4 \text{ M}^{-1}$ and $4.80 \times 10^4 \text{ M}^{-1}$ in silver nanoparticles prepared by magnetic stirrer and ultrasonic field respectively. The linearity of the Stern–Volmer plot indicates that only one type of quenching occurs in the system. In this case there is no possibility of formation of static quenching complexes between fluorophore–quencher pairs. Therefore collisional quenching is effectively possible.

The dependence of the fluorescence intensity upon quencher concentration is easily derived by consideration of the association constant for complex formation. In the present case the Benesi – Hildebrand approach was used to obtain the association constant. The association constant of silver nanoparticles prepared using magnetic stirrer and ultrasonic field method is $K_{ass} = 2159 \text{ M}^{-1}$ and 407 M^{-1} respectively from the plot of $[D]/\Delta A$ vs. $1/[Ag]$ (Figs. 12 and 13) where [Ag] is the concentration of silver, ΔA is the difference in absorbance value of silver nanoparticle solution and dye with silver nanoparticle solution and [D] is the concentration of NMTHN. The observed association constants indicate the presence of strong association between the silver nanoparticles and NMTHN.

Conclusion

The silver nanoparticles were prepared and the size of the silver nano particles has been calculated. The optical properties of NMTHN on silver nanoparticles are well studied using the absorption and fluorescence emission techniques. The fluorescence quenching of NMTHN by silver nanoparticles indicates that collisional quenching is effectively possible. The NMTHN molecules which are adsorbed on the surface of the silver nanoparticle leads to quenching of fluorescence.

Acknowledgement One of the authors (VR) is thankful to CSIR, Government of India for the financial assistance provided in the form of a research project. The author (PMK) is very thankful to UGC, Government of India for providing research fellowship in sciences for meritorious students.

References

1. Rusay RJ (1981) United States patent 19, July 7
2. Joshaghani M, Gholivand MB, Ahmadi F (2008) Spectrochim Acta A 70:1073
3. Rao PV, Rao CP, Wegelius E, Riesanen K (2003) J Chem Cryst 33:139
4. Fernandez-G JM, Rio-Portilla FD, Quiroz-Garcia B, Toscano RA, Salcedo R (2003) J Mol Struc 561:197
5. Solomon SD, Bahadory M, Jeyarajasingam AV, Rutkowsky SA, Boritz C (2007) J Chem Edu 84:322
6. Rosi NL, Mirkin CA (2005) Chem Rev 105:1547
7. Alivisatos P (2004) Nat Biotechnol 22:47
8. Junior AM, Moisés de Oliveira HP, Gehlen MH (2003) Photochem Photobiol Sci 2:921
9. Chatterjee S, Nandhi S, Bhattacharya SC (2005) J Photochem Photobiol A Chem 173:221
10. Creighton JA, Blatchford CG, Albrecht MG (1979) J Chem Soc Faraday Trans 2 75:790

11. Makarova OV, Ostafin AE, Miyoshi H, Norris JR Jr, Meisel D (1999) *J Phys Chem B* 103:9080
12. Taleb A, Petit C, Pileni MP (1998) *J Phys Chem B* 102:2214
13. Valmalette JC, Lemaire L, Hornyak GL, Dutta J, Hofmann H (1996) *Anal Mag* 24:m23
14. Pileni MP (1998) *New J Chem* 693
15. Demas JN, Crosby GA (1971) *J Phys Chem* 75:991
16. Umadevi M, Vanelle P, Terme T, Rajumar BJM, Ramakrishnan V (2009) *J Fluoresc* 19:3
17. Link S, El-Sayed MA (1999) *J Phys Chem B* 103:4212
18. Geddes CD, Cao H, Gryczynski I, Gryczynski Z, Fang J, Lakowicz JR (2003) *J Phys Chem A* 107:3443
19. Gust D, Moore TA, Moore AL (1993) *Acc Chem Res* 26:198
20. Avouris P, Persson BNJ (1984) *J Phys Chem* 88:837
21. Amihod D, Katz E, Willner I (1995) *Langmuir* 11:1313
22. Hu J, Zhang J, Liu F, Kittredge K, Whitesell JK, Fox MA (2001) *J Am Chem Soc* 123:1464
23. Lahav M, Gabriel T, Shipway AN, Willner I (1999) *J Am Chem Soc* 121:258
24. Huang T, Murray RW (2002) *Langmuir* 18:7077